Surface extended energy-loss fine structure spectroscopy: extraction of structural information from spectra recorded in the second derivative mode of the electron yield

1991 J. Phys.: Condens. Matter 3 5693

(http://iopscience.iop.org/0953-8984/3/30/003)

J. Phys.: Condens. Matter 3 (1991) 5693–5709. Printed in the UK

Surface extended energy-loss fine structure spectroscopy: extraction of structural information from spectra recorded in the second derivative mode of the electron yield

J Lopez, J Rousseau, J C Le Bosse and M Rjeb

Laboratoire de Physique des Interfaces et de Mécanique des Couches Minces†, Université Claude Bernard Lyon I, bât. 203, 69622 Villeurbanne Cédex, France

Received 25 October 1990

Abstract. In this paper we reinvestigate the relation between the Fourier transform of SEELFS (surface extended energy-loss fine structure spectroscopy) data recorded in the second derivative mode of the electron yield, and the radial distribution function $F(R)$ of atoms around the emitter. This relation is not obvious since the Fourier transform is done over wavevector modulus and the derivation is done with respect to energy. We show that, providing a k^3 weighting factor is introduced, an EXAFS-like (extended x-ray absorption fine structure) analysis leads to $R^2F(R)$ with a good accuracy. This gives an *a posteriori* justification of the treatment currently used in the literature. The reasoning is easily extended to the case of data recorded in the first derivative mode, for which $RF(R)$ is obtained with a k^2 weighting factor. It is also shown that the R^2 (respectively R) factor must be eliminated to obtain shell positions with good accuracy, which is generally not achieved in previous work. All these conclusions are supported by a numerical analysis performed in the case of a model spectrum associated with the Ni(1 1 1) M_{23} loss spectra.

1. Introduction

Surface extended energy-loss fine structure spectroscopy (SEELFS) has been widely used to obtain structural information upon surfaces (see for instance De Crescenzi (1985, 1987), De Crescenzi and Chiarello (1985) and also most of the papers listed in the references). The surface sensitivity of this technique is due to the use of an electron scattering reflection mode analogous to surface extended x-ray absorption fine structure (SEXAFS), but avoiding synchrotron radiation. The possibility of using basic laboratory commercial equipment (essentially Auger spectrometers) to perform SEELFS analysis has largely favoured the success of this EXAFS-like technique. However, SEELFS usefulness is not clearly established, although some attempts have been made in this way (Idzerda *et al* 1985, Stern 1986, Mila and Noguera 1986, 1987, Chainet 1987). For instance, questions concerning angular dependence of fine structures, multiple scattering effects in the near-edge region, interference between close edges, accurate determination of phase shifts

† This laboratory is dependent on the Ecole National Ingénieur Saint-Etienne (ENISE) and on the Université Claude Bernard Lyon (UCBL).

0953-8984/91/305693 + 17 $03.50

for shallow core levels and influence of the use of second derivative data measurements have to be carefully investigated. So the real interest in this method presupposes that a convincing data treatment has been established, in order to achieve accurate structural parameter determination.

Obviously it would be difficult to examine here all the previous points. So, in this paper, we are essentially concerned with the latter. The first important question that must be asked is: what is truly measured in SEELFS experiments? Usually they are performed in the second derivative mode by using a cylindrical mirror analyser (CMA). Then, it is well known that the measured quantity is proportional to $d^2[E_c I(E_c)]/dE_c^2$, where E_c is the kinetic energy and $I(E_c)$ the intensity associated with the electrons backscattered at the surface. Because of the factor E_c, coming from the response function of the analyser, this quantity does not seem to present great interest. Fortunately, the second derivative $d^2I(E_c)/dE_c^2$, which is the starting point of all data treatments, can be extracted from the previous quantity. A demonstration of this non-obvious property is given in appendix 2 and supported by a simulation of a Ni(111) M_{23} SEELFS-like spectrum. This simulation of a SEELFS experiment, developed in appendix 1 on the basis of an EXAFS-like formulation, clearly appears to be the only possibility for understanding the properties of SEELFS spectra and for checking the accuracy of their numerical treatments. However, some comments are necessary since no SEELFS theory is available for quantitative purposes. We are not interested in a direct comparison between theory and experiment. We only need a qualitative description of SEELFS data. We shall see in the next section that recent work gives some justification for the use of an EXAFS-like formulation, which is exactly what we need in the frame of our qualitative approach.

Another consequence of the lack of a quantitative SEELFS theory is that the only possibility to extract structural information contained in $d^2I(E_c)/dE_c^2$ is to use a Fourier transform (FT) method, since a direct comparison between theory and experiment is impossible. The situation is similar to EXAFS when theoretical phase shifts and backscattering amplitudes are not available. Such a FT is necessarily done over the backscattered electron wavevector modulus k, which is connected to the kinetic energy E_c by the relation

$$E_c = E_{\text{primary}} - E_{\text{threshold}} - k^2$$

where k^2 is the loss energy (in rydberg atomic units) referenced at the core edge energy $E_{\text{threshold}}$. Then, a difficulty arises: what is the relation between the second derivative of $I(E_c)$ with respect to the kinetic energy and the EXAFS-like radial distribution function $F(R)$ defined as the FT of $I(E_c(k))$ after some numerical pretreatments such as background elimination, restriction of the energy range, introduction of a weighting factor k^n (with n in the range 1 to 4), . . . ? Curiously, previous works were very reserved about this point. They implicitly assume, without any justification, that this FT is proportional to $R^2F(R)$. This property would be true if the derivation were performed with respect to the variable k, but in our situation, where the derivation is performed with respect to E_c, we cannot use any standard Fourier analysis theorem. So the principal aim of this paper is to elucidate this important point and to justify the relation used *a priori* in the literature.

In section 2, the way in which significant physical information can be extracted from SEELFS measurements will be carefully examined. Then, in section 3, a detailed Fourier analysis of SEELFS data will elucidate all the unsolved problems concerning this point. To confirm these theoretical results, a calculation, based upon a simulated spectrum, will be developed in section 4. Consequences concerning the validity of experimental

results previously reported in the literature will also be developed in this section. To close this work, a short conclusion will collect the main results in section 5.

2. Extraction of physical information from SEELFS measurements

The SEELFS theory is not so well established as the EXAFS one. Nevertheless, a recent analysis shows that, within the single-scattering approximation, the detected intensity appears as the product of a slowly varying matrix element multiplied by two oscillatory factors, the first of which is similar to EXAFS (Mila and Noguera 1986, 1987, Derrien *et al* 1987). Fortunately, it has also been shown in these papers that, in most experimental situations, EXAFS oscillations are not significantly perturbed by the second factor. Within this approximation SEELFS spectra can be treated using the formalism valid for EXAFS. Thus the oscillating part of the spectrum above a core edge is given by the usual formula written here for the K edge case:

$$\chi(k) = \sum_j \frac{N_j}{kR_j^2} A_j(k) \sin[2kR_j + \varphi_j(k)] \exp(-2\sigma_j^2 k^2) \times \exp[-2R_j/\lambda(k)] = \sum_j \chi_j(k) \tag{1}$$

where $\chi(k)$ is the relative change of the backscattered intensity $(I - I_0)/I_0$ similar to the EXAFS relative change of the absorption coefficient $(\mu - \mu_0)/\mu_0$, k is the wavevector modulus of the ejected electron, N_j is the number of equivalent atoms in the jth shell surrounding the emitting atom, R_j is the corresponding distance, $A_j(k)$ is the backscattering amplitude of atoms on the jth shell, $\varphi_j(k)$ is the total phase shift experienced by an electron during its path, σ_j is the Debye–Waller coefficient depending on both adsorber and backscatterer atoms of j type and $\lambda(k)$ is the mean free path of the ejected electron.

Previously such a relation has been widely used in SEELFS analysis (see for instance De Crescenzi *et al* (1983a), De Crescenzi and Chiarello (1985), Papagno and Caputi (1984) and also most of the papers listed in the references). We are not interested here in a quantitative simulation of SEELFS data. We only need an algebraic expression, qualitatively describing a SEELFS signal, to test the numerical treatment of a hypothetical experiment. On the basis of the above discussion, it can be argued that the fundamental EXAFS relation is accurate for this purpose.

As mentioned in the introduction, SEELFS data correspond to $d^2I(E_c)/dE_c^2$. We are not interested in the function $I(E_c) = I(E_{primary} - E_{threshold} - E)$, but in $I(E_c(E))$, $E = k^2$ being the loss energy. In order to simplify notation, the function $I(E_c(E))$ will be called $I(E)$ in further developments. With this new notation, $I(E)$ corresponds to the EXAFS function $\mu(E)$ (see appendix 2). Then SEELFS surface backscattered intensity $I(E)$, which becomes the starting point of data treatments, can be separated into two terms

$$I(E) = I_1(E) + I_2(E) \tag{2}$$

where $I_1(E)$ represents the background intensity not involved in the core edge excitation. It appears that the order of magnitude of $I_1(E)$ can be several hundred times the intensity change $I_2(E)$ due to this excitation. For this reason SEELFS spectra are generally recorded

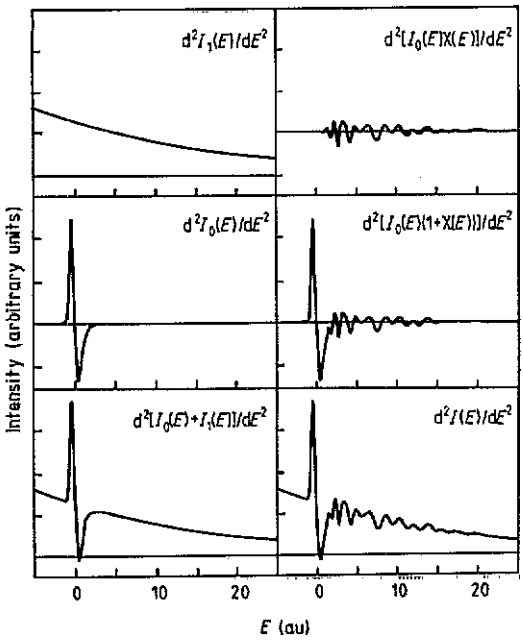

Figure 1. Graphical representation of the different terms occurring in $d^2I(E)/dE^2$ for the Ni(111) M_{23} threshold SEELFS model spectrum built in appendix 1.

in the first- or second-order derivative mode. The intensity $I_2(E)$ and $\chi(E)$ are now related by

$$I_2(E) = I_0(E)[1 + \chi(E)] \tag{3}$$

in which $I_0(E)$ would be the intensity backscattered by isolated atoms.

We can now use relations (2) and (3) to decompose the second derivative $d^2I(E)/dE^2$ into a sum of three terms:

$$\frac{d^2I(E)}{dE^2} = \frac{d^2I_1(E)}{dE^2} + \frac{d^2I_0(E)}{dE^2} + \frac{d^2[I_0(E)\chi(E)]}{dE^2}. \tag{4}$$

Using the model spectrum introduced in appendix 1, the behaviour of these three terms is illustrated on figure 1. The first one, $d^2I_1(E)/dE^2$, which is not oscillating, can be eliminated by some smoothing technique. Except in the near-edge region, the second one, $d^2I_0(E)/dE^2$, is negligible and can be eliminated by using an appropriate window. Thus, it can be concluded that the quantity $d^2[I_0(E)\chi(E)]/dE^2$ can be extracted with good accuracy from experimental data. Let us remark that the contribution of the intensity $I_0(E)$ cannot be eliminated from the previous quantity, because of the derivation.

To go further in the interpretation of SEELFS spectra, we now have to investigate what kind of structural information can be derived from the function $d^2[I_0(E)\chi(E)]/dE^2$. This is the aim of the next section.

3. Extraction of structural information from the function $d^2[I_0(E)\chi(E)]/dE^2$

In the absence of information about $I_0(E)$, the structural information contained in $d^2[I_0(E)\chi(E)]/dE^2$ can only be obtained by using a Fourier transform (FT) method.

Thus, following the standard EXAFS procedure, the quantity $I_0(E(k))\chi(E(k))$ is written down as a sum of neighbouring shell contributions:

$$I_0(k)\chi(k) = \sum_j g_j(k)\chi_{0j}(k) \tag{5}$$

with

$$\chi_{0j}(k) = N_j \sin[2kR_j + \varphi_j(k)] \exp(-2\sigma^2 k^2)/kR_j^2 \tag{6}$$

$$g_j(k) = I_0(k)A_j(k) \exp[-2kR_j/\lambda(k)]. \tag{7}$$

In these relations, the functions $I_0(E(k))$ and $\chi(E(k))$ are improperly called $I_0(k)$ and $\chi(k)$ to simplify the notation. Then, the FT of the contribution of the jth shell weighted by k is

$$k\chi_{0j}(k)g_j(k) \Leftrightarrow F_j(R) * G_j(R) \tag{8}$$

where the notations $\Leftrightarrow$ and $*$ respectively stand for the FT and the convolution product. Here

$$k\chi_{0j}(k) \Leftrightarrow F_j(R) \tag{9}$$

$$g_j(k) \Leftrightarrow G_j(R). \tag{10}$$

Generally, $g_j(k)$ is a bell-shaped function, only giving rise to a broadening of structures in R space. Thus all the physical information is contained in $F_j(R)$. A detailed analysis of this function is displayed in appendix 3. This analysis shows that $|F_j(R)|$ can be considered as a radial distribution function (RDF) associated with the jth shell. Obviously this is a well known result, even if the derivation presented in this appendix gives some new information, such as the slowly asymptotic decrease as $1/|R - R_j^*|$ of $|F_j(R)|$, where R_j^* is the effective location of the jth shell including phase shift correction (see appendix 3).

For any shell, by derivation of (8), the classical Fourier analysis gives

$$\frac{\mathrm{d}}{\mathrm{d}k}[k\chi_{0j}(k)g_j(k)] \Leftrightarrow 2\mathrm{i}R[F_j(R) * G_j(R)] \tag{11}$$

$$\frac{\mathrm{d}^2}{\mathrm{d}k^2}[k\chi_{0j}(k)g_j(k)] \Leftrightarrow -4R^2[F_j(R) * G_j(R)]. \tag{12}$$

Unfortunately, the quantity that can be extracted from a SEELFS experiment has nothing to do with (11) or (12) since the experimental set-up implies first- or second-order derivatives upon energy and not upon wavevector. Nevertheless, it can easily be shown that

$$4k^3 \frac{\mathrm{d}^2}{\mathrm{d}E^2}[I_0(k)\chi_j(k)] + 6k \frac{\mathrm{d}}{\mathrm{d}E}[I_0(k)\chi_j(k)] \Leftrightarrow -4R^2[F_j(R) * G_j(R)]. \tag{13}$$

This relation can be modified, giving rise to

$$k^3 \frac{\mathrm{d}^2}{\mathrm{d}E^2}[I_0(k)\chi_j(k)] \Leftrightarrow -R^2\left([F_j(R) * G_j(R)] + \frac{3\mathrm{i}}{2R}[F_j(R) * G_j^{[1]}(R)]\right) \tag{14}$$

where $G_j^{[1]}(R)$ is defined by the relation

$$g_j(k)/k \Leftrightarrow G_j^{[1]}(R). \tag{15}$$

Let us remark that the apparent singularity of $g_j(k)/k$ at 0 is unimportant because, in practice, $g_j(k)$ always implies a window function that collapses the k region near 0.

In the right-hand side of (14), the second term is expected to be negligible compared with the first one because:

(i) the factor $3/2R$ is small, even for the first shell radius;

(ii) $G_j^{[1]}(R)$ is lower than $G_j(R)$ since $g_j(k)/k$ is lower than $g_j(k)$ within the integration domain (in most cases, the region $k < 1$ is strongly lessened by the apodization process).

Moreover, let us note that, because of the factor i, there is a great tendency to quadrature between the two terms of the sum on the right-hand side of (14). Thus, the contribution of the second term to the modulus of the sum is even smaller.

From this algebraic analysis, it can be concluded that *the use of a k^3 weighting factor allows an EXAFS-like analysis for SEELFS spectra recorded in the second derivative mode, leading to $R^2F(R)$* instead of the complete radial distribution function $F(R)$, which is defined as

$$F(R) = \left| \sum_j F_j(R) * G_j(R) \right|. \tag{16}$$

So far, we have only discussed the analysis of experiments recorded in the second derivative mode. However, the first derivative mode is sometimes used. In the same way it can easily be shown that

$$k^2 \frac{\mathrm{d}}{\mathrm{d}E}[I_0(k)\chi_j(k)] \Leftrightarrow \mathrm{i}R\left([F_j(R) * G_j(R)] + \frac{\mathrm{i}}{2R}[F_j(R) * G_j^{[1]}(R)]\right). \tag{17}$$

Thus, using the same arguments as previously, it follows that the last term in the right-hand side of (17) can be neglected. So $R\,|F(R)|$ *can be obtained from SEELFS data recorded in the first derivative mode with the use of a k^2 weighting factor.*

These results give a theoretical justification for the choice of the weighting factor exponent value. Weighting of data by a factor k^n, where $0 \leqslant n \leqslant 3$, has been routinely used in SEELFS without reference to a theoretical analysis. In the case of second-order derivative measurements, a tedious but straightforward calculation leads to the general result that

$$k^n \frac{\mathrm{d}^2}{\mathrm{d}E^2}[\chi_j(k)I_0(k)] \Leftrightarrow -R^2[F_j(R) * G_j^{[3-n]}(R)] + \mathrm{i}R(\tfrac{3}{2} - n)[F_j(R) * G_j^{[4-n]}(R)] + \tfrac{1}{4}(n^2 - 4n + 3)[F_j(R) * G_j^{[5-n]}(R)] \tag{18}$$

where

$$g_j(k)/k^p \Leftrightarrow G_j^{[p]}(R). \tag{19}$$

The singularity of $g_j(k)/k^p$ near 0 is unimportant for reasons discussed above in the particular case $n = 1$. Obviously, the previous discussion of (14) holds for (18), which approximately reduces to

$$k^n \frac{\mathrm{d}^2}{\mathrm{d}E^2}[\chi_j(k)I_0(k)] \Leftrightarrow -R^2[F_j(R) * G_j^{[3-n]}(R)]. \tag{20}$$

A similar result would be obtained for first-order derivative measurements. Thus, it can be concluded that *the use of a k^n weighting factor with n different from the theoretical value is essentially equivalent to a change in the convolution function.*

Let us now remark that two main effects are induced by the division of $g_j(k)$ by k^n: a reduction of the amplitude of this function and a reduction of its width. The first effect has previously been put forward to justify the negligible character of correction terms occurring in (14) as well as in (18). The second leads to an increase in the peak resolution of $F(R)$ when n becomes greater, which is an interesting effect.

To close this section, let us remark that the results derived above do not make use of any explicit algebraic form for $\chi(k)$. The only assumption is that $I_0(k)\chi(k)$ may be considered as a sum of shell contributions (see relation (3)), the FT of which are connected with the RDF associated with these shells. Obviously, this is the *a priori* assumption of SEELFS, so that our results are valid, except if all the basic ideas at the origin of SEELFS break down.

4. Model calculation

Following ideas developed in section 2, the previous algebraic results are tested on the basis of a model calculation. This is the only way to be sure that a restitution of the RDF from the second derivative of the electron yield versus energy is really satisfactory. The construction of the SEELFS model spectrum used throughout this section (corresponding to the Ni(1 1 1) M_{23} threshold) is detailed in appendix 1.

4.1. Degree of restitution of the RDF from relation (14)

In a first stage, let us only consider the first shell. The reference RDF is the FT of the first shell contribution without derivation versus energy (FT$[kI_0(k)\chi_1(k)]$). This reference RDF is represented by the full curve on figure 2(a). According to the previous discussion of (14), the quantity

$$\frac{1}{R^2}\left|\mathrm{FT}\left(k^3\frac{\mathrm{d}^2}{\mathrm{d}E^2}[I_0(k)\chi_1(k)]\right)\right|$$

would give a good approximation of this RDF. This conclusion is supported by the result of the computation, which is represented by crosses on figure 2(a). The second term of (14):

$$\frac{3}{2R^3}\left|\mathrm{FT}\left(k\frac{\mathrm{d}}{\mathrm{d}E}[I_0(k)\chi_1(k)]\right)\right|$$

is also represented on this figure (dotted curve). Its expected very weak influence after recombination with the first term is well verified. The reason is that the phase shift between these two terms is near $\pi/2$. This point is illustrated on figure 3.

Extension of this analysis to the first nine shells sustains the above conclusion (figure 2(b)). Let us remark that the contribution of the second term in (14) becomes negligible for R values above the first shell range. This is essentially due to the supplementary factor $1/R$, which lessens the contribution of the outermost shells.

4.2. Influence of the R^2 factor on the RDF peak positions

The FT of spectra recorded in the second derivative mode corresponds to the RDF $F(R)$ plus an extra factor R^2 (see (14)) generally denoted $\tilde{F}(R)$. So, to get the true RDF peak

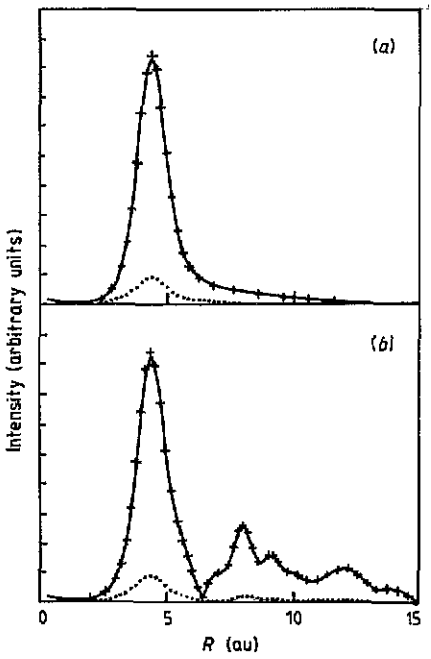

Figure 2. RDF contribution of the two terms occurring in (14). Figures (*a*) and (*b*) respectively correspond to computations including the first shell and nine shells. Full curve: FT$[k\chi_1(k)I_0(k)]$ reference FT associated with an EXAFS-like computation.
Crosses: $(1/R^2)|\text{FT}\{k^3(\mathrm{d}^2/\mathrm{d}E^2)[I_0(k)\chi(k)]\}|$.
dotted curve: $(3/2R^2)|\text{FT}\{k(\mathrm{d}/\mathrm{d}E)[I_0(k)\chi(k)]\}|$.

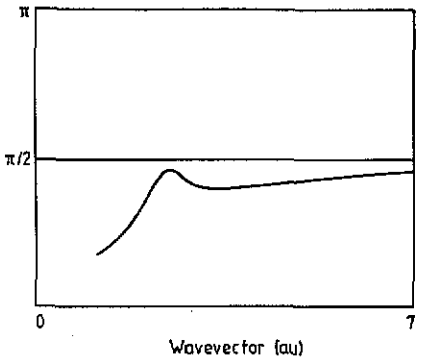

Figure 3. Phase shift between FT of the two terms on the left of (13):

$$\text{Arg}[\text{FT}\{k^3(\mathrm{d}^2/\mathrm{d}E^2)[I_0(k)\chi_1(k)]\}] - \text{Arg}[\text{FT}\{k(\mathrm{d}/\mathrm{d}E)[I_0(k)\chi_1(k)]\}].$$

This phase shift is very close to the one between the two terms on the right of (14) since in both cases the second terms are negligible compared with the first ones.

positions, the FT of SEELFS data must be divided by R^2, which has been done in the previous section. However, as noted by Hitchcock and Teng (1985), the $1/R^2$ correction has not been systematically applied to analyse SEELFS spectra (Rosei *et al* 1983, Polizzi *et al* 1984, Chiarello *et al* 1984, De Crescenzi and Chiarello 1985). Such omission leads to an artificial enhancement of the large-R features and is able to introduce an important shift of peak positions.

De Crescenzi and Chiarello (1985) have tried to justify that peak positions remain unaffected by the R^2 factor. Starting from an EXAFS-like Ni K edge spectrum, they observe that the $F(R)$ and $\tilde{F}(R)$ curves, respectively deduced from the initial spectrum and after a double derivative procedure, are peaked at nearby R values. Their conclusion seems more especially convincing as it is observed with relatively sharp peaks. Unfortunately, the situation is often different in SEELFS inasmuch as the short width of the investigated energy range induces a broadening of the RDF peaks.

To clarify this point, we study the influence of the R^2 factor included in $\tilde{F}(R)$, according to a theoretical approach. Let us describe a peak occurring in $\tilde{F}(R)$ by a Gaussian curve peaked at R_0:

$$\tilde{F}(R) = K\exp\{-[(R - R_0)/a]^2\} \tag{21}$$

and consider the function $F(R) = \tilde{F}(R)/R^2$. The calculation of the $F(R)$ derivative shows that the new maximum R_M, which corresponds to

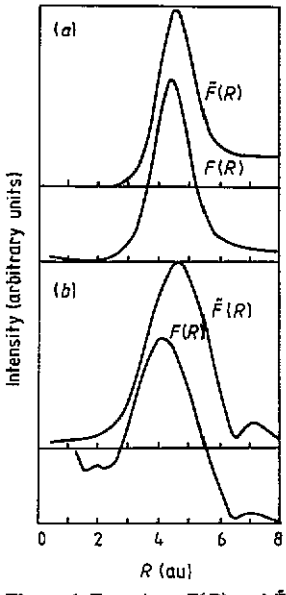

Figure 4. Functions $F(R)$ and $\tilde{F}(R)$ corresponding to the model spectrum reduced to the contribution of the first shell: (*a*) computation without reduction of the wavevector range; (*b*) computation after reduction of the wavevector range from 3 to 7.5 Å^{-1}.

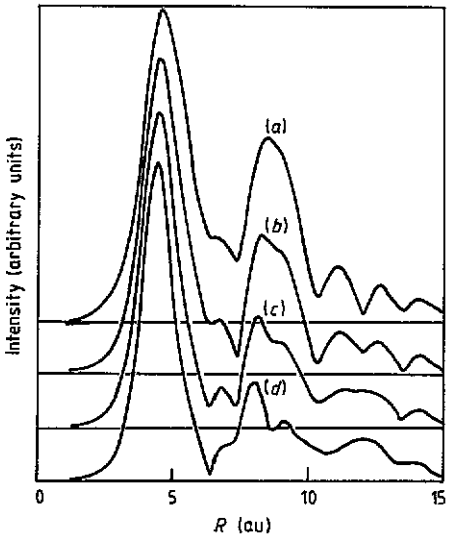

Figure 5. Functions $F(R)$ deduced from the model spectrum for different powers of the weighting factor k^n: (*a*) $n = 0$; (*b*) $n = 1$; (*c*) $n = 2$; (*d*) $n = 3$.

$$R_M = \tfrac{1}{2}R_0[1 + (1 - 4a^2/R_0^2)^{1/2}] \tag{22}$$

is systematically shifted down. This displacement depends upon the parameter a, which is connected to the full width at half-maximum (FWHM) $\Delta R = 2a(\log 2)^{1/2}$ of the Gaussian peak. So, R_M can be expressed in terms of ΔR as

$$R_M = \tfrac{1}{2}R_0\{1 + [1 - (\Delta R)^2/(R_0^2 \log 2)]^{1/2}\}. \tag{23}$$

For sharp Gaussian peaks, $\Delta R \ll R_0$ and we have

$$R_M - R_0 \simeq -R_0(\Delta R/R_0)^2/(4 \log 2). \tag{24}$$

The peak displacement is all the more negligible as the ratio $\Delta R/R_0$ and the distance R_0 are small. Unfortunately, for SEELFS spectra, the ratio $\Delta R/R_0$ is not small in the case of the first shell.

This point is illustrated in the case of the Ni(1 1 1) M_{23} threshold. We evaluate peak displacements induced by substituting $\tilde{F}(R) = R^2F(R)$ for $F(R)$. Four situations have been examined:

(i) The RDF published by Rosei *et al* (1983), where the $\tilde{F}(R)$ peaks are large because of the small integration range used for the Fourier transform (3–7.5 Å^{-1}); then the shift deduced from (23) is about 0.6 Å.

(ii) The RDF published by De Crescenzi *et al* (1981), which also presents large peaks, for the same reason. The shift deduced from (23) is about 0.4 Å.

(iii) The RDF corresponding to our model spectrum, for which the shift observed after division of $\tilde{F}(R)$ by R^2 (0.09 Å) is close to the estimated shift (0.08 Å) deduced

from (23) (see figure 4(*a*)). Let us remark that these shifts are very much lower than the previous ones because the integration range was not limited.

(iv) The RDF deduced from the previous theoretical spectrum after a reduction to the range 3–7.5 $Å^{-1}$, which is reported on figure 4(*b*). In this case, the shift observed after division of $\tilde{F}(R)$ by R^2 becomes important (0.24 Å) and is quite similar to the shift estimated from (23).

From this analysis, it can be concluded that it is probably not possible to determine peak positions from $\tilde{F}(R)$. However, a difficulty arises: the division of $\tilde{F}(R)$ by R^2 is not easy to realize (from a numerical point of view). More precisely, such a division can only be performed if the function $\tilde{F}(R)$ is very weak near $R = 0$. Obviously this property is connected with very good elimination of the background from measurements, which is a difficult problem.

To close this section, let us remark that the first shell positions, deduced from the two experiments reported above, are about 1 Å lower than the real one when they are evaluated from (23). This important shift cannot be explained on the basis of our actual knowledge of the M_{23} phase shift behaviour, which is generally replaced by the L_{23} ones (Ekardt and Tran Thoai 1983).

4.3. Influence of the k^n weighting factor

The choice of n for the k^n weighting factor seems very confused in the literature on SEELFS studies. In many papers, the presence of a weighting factor is not mentioned all through the numerical treatments and probably data recorded in first or second derivative mode are not weighted (see for instance Atrei *et al* 1989, Papagno and Caputi 1984, Papagno *et al* 1986, De Crescenzi 1985, De Crescenzi *et al* 1982, 1984, 1987, 1989, Chainet *et al* 1986, Chiarello *et al* 1984, Polizzi *et al* 1984, Rosei *et al* 1983, Idzerda *et al* 1987a, b, Caputi *et al* 1987). In some papers second derivative SEELFS data are only weighted by k (see Atrei *et al* 1987a, b, Tyliszczak and Hitchcock 1986, Papagno *et al* 1982) or k^2 (De Crescenzi 1987). Sometimes the k^n weighting factor is mentioned, but without the indication of the n value (De Crescenzi *et al* 1981, 1983b). However, correct n values are used in several papers, that is to say 2 in the case of SEELFS data recorded in the first derivative mode (Teng and Hitchcock 1983, Hitchcock and Teng 1985, Natarajan *et al* 1985, Idzerda *et al* 1985, 1987a, b) and 3 when the second derivative mode is used (De Crescenzi and Chiarello 1985).

To clarify the influence of the k^n weighting factor on the RDF peaks, we have calculated the RDF with different n values, from the SEELFS model spectrum associated with the Ni(1 1 1) M_{23} edge. Results obtained with $n = 0$, 1, 2 and 3 are reported on figure 5. In agreement with the algebraic results reported in section 3, we observe a better resolution of the RDF peaks when n increases. Moreover, the location of the first peak is very weakly affected by a change in the n value, which is an interesting result.

5. Conclusions

In this paper we have mainly studied the relation between the Fourier transform of SEELFS spectra recorded in the second derivative mode and the RDF. On the basis of an algebraic study, we have shown that, with a k^3 weighting factor, an EXAFS-like analysis leads to $\tilde{F}(R) = R^2F(R)$ with good accuracy. This result, which is supported by a computation based upon a model spectrum corresponding to the Ni(1 1 1) M_{23} threshold,

appears as an *a posteriori* justification of the numerical treatments previously used in the literature devoted to SEELFS.

We also elucidate the question concerning the choice of the exponent of the weighting factor k^n, introduced just before the FT calculation. Let us recall that values $n \neq 3$ are often used in previous work. This is not a side issue, because a weighting of $d^2[I_0(k)\chi(k)]/dE^2$ cannot be assimilated to a weighting of $I_0(k)\chi(k)$. We show that the choice of n value different from 3 essentially corresponds to a change in the convolution function, which distorts the RDF. In that sense, no drastic modifications in the physical results are induced by a change in the power of the k^n weighting factor. This result is also an *a posteriori* justification of previous SEELFS spectra treatments. On the basis of our model spectrum, it can be argued that the use of n values greater than the theoretical one does not significantly shift peak positions, but leads to a better peak resolution, which is an interesting result.

All these conclusions are easily extended to the case where data are recorded in the first derivative mode, which happens sometimes. The only difference is that $\tilde{F}(R)$ becomes $RF(R)$ instead of $R^2F(R)$, with the help of a k^2 weighting factor instead of a k^3 weighting factor.

Let us now come back to the procedure in which peak shell positions are generally determined from $\tilde{F}(R)$. For undetermined reasons, in previous work, the extra factor R^2 has not been eliminated in $\tilde{F}(R)$. On the basis of the analysis developed in section 4.2, it can be concluded that shell positions deduced from $\tilde{F}(R)$ instead of $F(R)$ are much more sensitive to the presence of the additional R^2 factor than to the power of the weighting factor. In the case of the Ni(1 1 1) M_{23} threshold, evaluation of this effect, on the basis of experimental $\tilde{F}(R)$ curves reported in the literature, leads to a lowering of the first shell position up to 0.6 Å. This result clearly invalidates most of the conclusions of previous work and necessarily implies a new insight in the interpretation of SEELFS data. The problem emerging from this result concerns the accuracy of the M_{23} phase shift determination. This is a theoretical problem far away from the aim of the present paper, but some progress in this field is required.

To conclude, let us emphasize that this paper constitutes a well defined theoretical framework to understand numerical treatments of SEELFS spectra. Other problems associated with these numerical treatments, such as the control of background removal or the effects connected with spectra truncation, have been intentionally forgotten in this paper. They will be the subject of a forthcoming paper.

Acknowledgments

We would like to thank Dr J C Bertolini and Dr B Tardy for helpful discussions. This work was developed in the frame of the scientific programme of the Groupement Surfaces Rhône-Alpes.

Appendix 1. Algebraic simulation of a Ni(1 1 1) M_{23} energy-loss spectrum

In this appendix we give information about the construction of the SEELFS model spectrum, which is used throughout the paper to test the results derived from algebra. We choose the Ni(1 1 1) M_{23} energy-loss spectrum because it has been widely studied in the literature (De Crescenzi *et al* 1981, Rosei *et al* 1983, Hitchcock and Teng 1985, De

Crescenzi and Chiarello 1985). A complete treatment of a corresponding experiment will be the subject of a forthcoming paper. According to the discussion of section 2, SEELFS oscillations will be obtained on the basis of the classical EXAFS formula. However, we first need expressions for $I_0(E)$ and $I_1(E)$.

Let us introduce the function $s(x, a)$ defined as

$$s(x, a) = \exp[-\exp(-ax)] \tag{A1.1}$$

which is nothing else than a smooth step function always presenting an inflection point at the origin. With the help of this function, we choose the following analytical form for $I_0(E)$:

$$I_0(E) = cs(E, a)\exp(-bE) \tag{A1.2}$$

where c, a and b are appropriate constants. Since M_{23} thresholds take place in the tail of the elastic peak, the intensity $I_1(E)$ is generally a decreasing function over all the experimental range. For the sake of simplicity we set

$$I_1(E) = \exp(-bE) \tag{A1.3}$$

with the same constant b, so that $I_0(E)$ can be written as

$$I_0(E) = cs(E, a)I_1(E). \tag{A1.4}$$

In these relations the origin of energy corresponds to the core edge.

We now need an algebraic expression for all the functions appearing in the fundamental EXAFS formula.

The backscattered amplitude $A(k)$ has often been represented by a simple Lorentzian (Teo *et al* 1977) or other expressions (Cramer *et al* 1976). A better approximation can be obtained on the whole spectrum as follows:

$$A(k) = s(k - k_1, A)A_0/\{1 + [A_2(k - k_0)]^2\} \tag{A1.5}$$

where A, A_0, A_2, k_0 and k_1 are constants.

The total phase shift function $\varphi(k)$ generally presents a linear behaviour on a large range. A very good fitting of this function can be obtained by setting

$$\varphi(k) = s(k - k_2, B)(B_1k + B_0) \tag{A1.6}$$

where B, B_0, B_1 and k_2 are other constants.

The Debye–Waller factor σ^2 is deduced from the Debye temperature θ_D on the basis of the relation

$$\sigma^2 = (6\hbar/m\omega_D)[1/4 + (T/\theta_D)^2\varphi] \tag{A1.7}$$

in which the displacement correlation function has been neglected (Beni and Platzman 1976), m is the mass of a nickel atom, $\omega_D = k_B\theta_D/\hbar$ and

$$\varphi = \int_0^{\theta_D/T} \frac{x}{\exp(x) - 1}\,dx. \tag{A1.8}$$

The variation of the electron mean free path $\lambda(k)$ with wavevector k is chosen of the form $\lambda(k) = k/\Gamma$ (Lee and Beni 1977), where the constant Γ can be derived from the electron mean free path universal curve.

Interatomic distances and number of neighbouring atoms on each shell are those of a surface atom located at an unrelaxed surface.

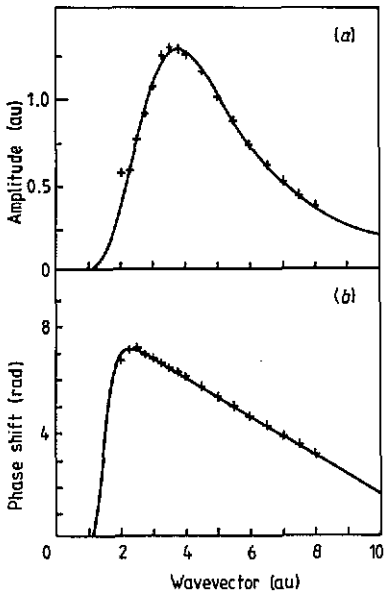

Figure A1. Backscattering amplitudes (*a*) and total phase shifts (*b*) for the Ni(111) M_{23} threshold. The crosses correspond to the values deduced from Teo and Lee's (1979) tables and the full curves are issued from the numerical optimization of parameters occurring in relations (A1.5) and (A1.6).

Finally, the SEELFS spectrum is directly obtained from two successive derivations of $I_1(E) + I_0(E)[1 + \chi(E)]$ versus E, where $E = k^2$.

In the case of the Ni(1 1 1) M_{23} threshold, we use the following set of parameters (in rydberg atomic units):

$I_0(E)$ and $I_1(E)$	$a = 2.397, b = 5 \times 10^{-2}, c = 2.8 \times 10^{-3}$
$A(k)$	$A_0 = 1.562, A_2 = 0.356, k_0 = 3.052, k_1 = 2.183, a = 1.284$
$\varphi(k)$	$B = 4.275, B_0 = 8.962, B_1 = -0.723, k_2 = 1.412$
σ^2	$\sigma^2 = 0.034\,823$
$\lambda(k)$	$\Gamma = 0.2573.$

Let us remark that the parameters concerning the functions $A(k)$ and $\varphi(k)$ have been obtained with the help of an optimization process from Teo and Lee's (1979) tables. The results concerning these two functions are reported on figure A1 where crosses indicate the values derived from Teo and Lee's tables. The total phase shift $\varphi(k)$ has been obtained on the basis of the standard approximation, which consists of replacing the M_{23} phase shift by the corresponding L_{23} phase shift (Ekardt and Tran Thoai 1983).

The reconstruction of the pseudo-experimental curve $d^2I(E)/dE^2$ from $d^2I_1(E)/dE^2$, $d^2I_0(E)/dE^2$ and $d^2[I_0(E)\chi(E)]/dE^2$ is presented on figure 1 and can be compared with previous reported experiments (see for instance De Crescenzi and Chiarello 1985). A more complete analysis of such a comparison will be discussed in a forthcoming paper.

Appendix 2

SEELFS spectra are generally collected with the help of a CMA, in which it is well known that the transmitted current $i(E_c)$ is proportional to the kinetic energy E_c according to the relation

$$i(E_c) = KE_cN(E_c). \tag{A2.1}$$

Here $N(E_c)$ is the intensity associated with the electrons backscattered at the surface. In practice, the detection of interesting features is considerably improved by the use of a lock-in amplifier, allowing one to get either $d[KE_cN(E_c)]/dE_c$ or $d^2[KE_cN(E_c)]/dE_c^2$. Since most measurements are performed in the second derivative mode, the quantity expected to be obtained is

$$\frac{d^2i(E_c)}{dE_c^2} = K\left(2\frac{dN(E_c)}{dE_c} + E_c\frac{d^2N(E_c)}{dE_c^2}\right). \tag{A2.2}$$

We are not interested in the function $i(E_c)$, but rather in the function $I(E) = N(E_p - E_0 - E)$, where E is the loss energy, referenced at the energy threshold E_0, and E_p is the energy of primary electrons†. It follows that

$$dN(E_c)/dE_c = -dI(E)/dE \tag{A2.3a}$$

$$d^2N(E_c)/dE_c^2 = d^2I(E)/dE^2. \tag{A2.3b}$$

Unfortunately, there is no reason that allows one to assert *a priori* that the first term on the right-hand side of (A2.2) is negligible. So the relation (A2.2) must be carefully investigated. From (2) and (3) it can be shown that

$$\frac{d^2[I(E_c)]}{dE_c^2} = K\left(-2\frac{d[I_1(E) + I_0(E)]}{dE} + E_c\frac{d^2[I_1(E) + I_0(E)]}{dE^2}\right.$$
$$\left. - 2\frac{d[I_0(E)\chi(E)]}{dE} + E_c\frac{d^2[I_0(E)\chi(E)]}{dE^2}\right). \tag{A2.4}$$

The two first terms on the right of (A2.4) are unimportant, even if they are not negligible, because they only correspond to an additional background easily eliminated during the numerical treatment of spectra. The only remaining problem is the relative importance of the third and the last terms. Obviously the oscillating behaviour of these two terms is controlled by the first and second derivatives of factors such as $\sin(2kR_j + \varphi)$ versus energy. It appears that last $E_c\,d/dE$ derivation introduces a factor $(E_c/E)kR_j$. Since this factor is very large compared with 1, because E_c/E as well as kR_j are large compared with 1 in all the experimental range, it can be concluded that all the oscillating behaviour of (A2.4) comes from the last term, which is a quite interesting result. It means that after division of SEELFS spectra by E_c, followed by some background subtraction and elimination of the near-edge region (with the help of a window function for instance), the remaining function is nothing else than $d^2[I_0(E)\chi(E)]/dE^2$, which is the expected result.

This conclusion is completely supported by a computation carried out on the basis of our model spectrum. The results are reported on figure A2. It clearly appears that the term $2\,dN(E_c)/dE_c$, appearing in (A2.2), only contributes to a modification of the background of $d^2[i(E_c)]/dE_c^2$. The oscillatory behaviour of $2\,dN(E_c)/dE_c$ is completely negligible at the scale of oscillations appearing in the term $E_c\,d^2N(E_c)/dE_c^2$. This numerical result is confirmed by a crude estimation of the factor $(E_c/E)kR_1$, which is greater than 50 for our model spectrum.

† In section 2 there is a slight confusion between the functions $N(E)$ and $I(E) = N(E_p - E_0 - E)$, which are both called $I(E)$. This subtlety, corresponding mathematically to a function change, is unimportant for the understanding of the general reasoning.

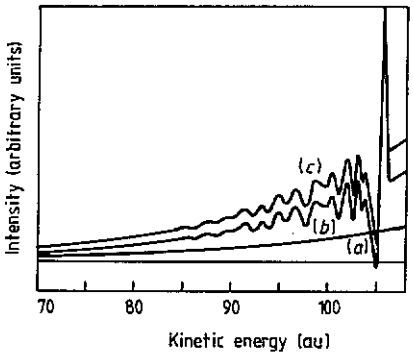

Figure A2. Numerical study of the two terms contributing to the intensity $i(E_c)$, according to the relation (A2.2): (*a*) $2\,\mathrm{d}N(E_c)/\mathrm{d}E_c$; (*b*) $E_c\,\mathrm{d}^2N(E_c)/\mathrm{d}E_c^2$; (*c*) $i(E_c) = 2\,\mathrm{d}N(E_c)/\mathrm{d}E_c + E_c\,\mathrm{d}^2N(E_c)/\mathrm{d}E_c^2$.

Appendix 3

The aim of this appendix is to study the algebraic properties of the FT of $k\chi_{0j}(k)$, with the notations used in section 3. Following the idea of Sayers *et al* (1971), we take the FT of the jth shell contribution to an EXAFS-like signal reduced to $\chi_{0j}(k)$ as

$$F_j(R) = \frac{1}{\pi^{1/2}} \int_{-\infty}^{\infty} k\chi_{0j}(k)\theta(k) \exp(-2ikR)\,\mathrm{d}k. \tag{A3.1}$$

Here, the step function $\theta(k)$ has been introduced because $\chi_{0j}(k)$ is only defined for positive values of k. The above FT can be written as the convolution product:

$$F_j(R) = \mathrm{FT}[k\chi_{0j}(k)] * \mathrm{FT}[\theta(k)]. \tag{A3.2}$$

Relation (A3.2) can be rewritten as

$$F_j(R) = \frac{\pi^{1/2}}{2} I_j(R) * \left[\delta(R) - \frac{i}{\pi}\mathrm{P}\left(\frac{1}{R}\right)\right] \tag{A3.3}$$

where $\delta(R)$ is the Dirac distribution, $\mathrm{P}(1/R)$ the principal part distribution and

$$I_j(R) = \frac{1}{\pi^{1/2}} \frac{N_j}{R_j^2} \int_{-\infty}^{\infty} \sin[2kR_j + \varphi_j(k)] \exp(-2\sigma_j^2 k^2) \exp(-2ikR)\,\mathrm{d}k. \tag{A3.4}$$

Using a linear approximation for the phase shift $\varphi_j(k)$:

$$\varphi_j(k) = -2kR_{0j} + \varphi_{0j} \tag{A3.5}$$

we obtain

$$I_j(R) = \frac{1}{\pi^{1/2}} \frac{N_j}{R_j^2} \int_{-\infty}^{\infty} \sin(2kR_j^* + \varphi_{0j}) \exp(-2\sigma_j^2 k^2) \exp(-2ikR)\,\mathrm{d}k \tag{A3.6}$$

where $R_j^* = R_j - R_{0j}$ is an effective distance between the emitting atom and the jth shell including a phase shift correction. Some straightforward calculations lead to

$$I_j(R) = \frac{\mathrm{i}}{2\pi^{1/2}} \frac{N_j}{R_j^2} [J_j^+(R) - J_j^-(R)] \tag{A3.7}$$

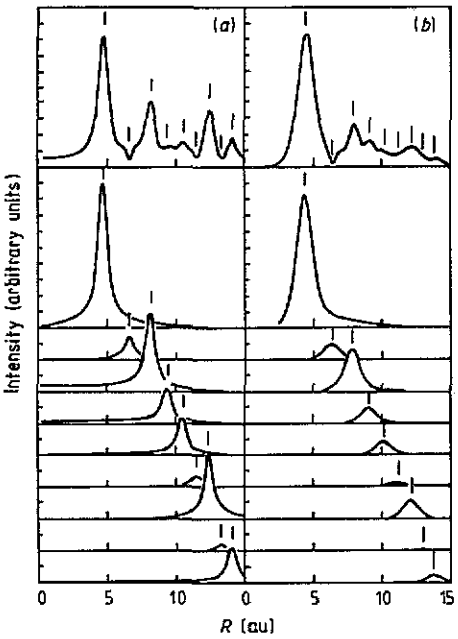

Figure A3. RDF associated with a Ni(111) surface atom: (*a*) $|\mathrm{FT}[kI_0(k)\chi(k)]|$ for the first nine shells and $|\mathrm{FT}[kI_0(k)\chi_j(k)]|$ for each shell in which $g_j(k)$ and $\varphi_j(k)$ (see (6) and (7)) are respectively replaced by 1 and 0; (*b*) $|\mathrm{FT}[kI_0(k)\chi(k)]|$ for the first nine shells and $|\mathrm{FT}[kI_0(k)\chi_j(k)]|$ for each shell without neglecting the influence of the previous factors. True positions of different shells are indicated by vertical marks.

with

$$J_j^{\pm}(R) = \exp(\pm i\varphi_{0j}) \int_{-\infty}^{\infty} \cos[2k(R \mp R_j^*)] \exp(-2\sigma_j^2 k^2)\, dk. \qquad (A3.8)$$

The above integral is known, so

$$J_j^{\pm}(R) = \pi \exp(\pm i\varphi_{0j}) f_j(R \mp R_j^*) \qquad (A3.9)$$

where $f_j(R)$ is the normalized Gaussian

$$f_j(R) = \exp[-R^2/(2\sigma_j^2)]/(2\pi\sigma_j^2)^{1/2}. \qquad (A3.10)$$

It is obvious to note that the contribution of the term proportional to $J_j^-(R)$ in (A3.7) is negligible, since it involves a Gaussian centred upon $-R_j^*$, which is a distance far out of the physical range.

Coming back to (A3.3) we obtain

$$F_j(R) = (\pi N_j/2R_j^2) \exp(i\varphi_{0j})\{\mathrm{HT}[f_j(R - R_j^*)] - i f_j(R - R_j^*)\} \qquad (A3.11)$$

so $F_j(R)$ is proportional to a function whose imaginary part is the opposite of a Gaussian centred at R_j^* and real part is the Hilbert transform (HT) of this Gaussian.

We are only interested in the modulus $|F_j(R)|$. Since $f_j(R - R_j^*)$ is even with respect to $R - R_j^*$ and, according to a well known property of the HT transform, $\mathrm{HT}[f_j(R - R_j^*)]$ is odd, it follows that $|F_j(R)|$ is an even function of $R - R_j^*$. Moreover, because of the presence of the HT of $f_j(R - R_j^*)$, this function behaves asymptotically as $1/(R - R_j^*)$. This demonstrates the algebraic properties of $F_j(R)$. All these results are summarized on figure A3. The comparison between figures A3(*a*) and A3(*b*) gives interesting indications upon the influence of the convolution factors $G_j(R)$ (see equation (8)).

References

Atrei A, Bardi U, Maglietta M, Rovida G, Torrini M and Zanazzi E 1989 *Surf. Sci.* **211–212** 93–7
Atrei A, Bardi U, Rovida G, Torrini M and Zanazzi E 1987a *Surf. Sci.* **189–190** 459–65
Atrei A, Bardi U, Rovida G, Torrini M, Zanazzi E and Maglietta M 1987b *J. Vac. Sci. Technol.* A **5** 1006–8
Beni G and Platzman B M 1976 *Phys. Rev.* B **14** 1514–18
Caputi L S, Chiarello G and Amoddeo A 1987 *Surf. Sci.* **188** 63–9
Chainet E 1987 *PhD Thesis* University of Grenoble
Chainet E, De Crescenzi M, Derrien J, Nguyen T T A and Cinti R C 1986 *Surf. Sci.* **168** 801–9
Chiarello G, Colavita E, De Crescenzi M and Nannarone S 1984 *Phys. Rev.* B **29** 4878–89
Cramer S P, Eccles T K, Kutzler F, Hodgson K O and Doniach S 1976 *J. Am. Chem. Soc.* **98** 8059–69
De Crescenzi M 1985 *Surf. Sci.* **162** 838–46
—— 1987 *J. Vac. Sci. Technol.* A **5** 869–74
De Crescenzi M, Antonangeli F, Bellini C and Rosei R 1983a *Solid State Commun.* **46** 875–80
—— 1983b *Phys. Rev. Lett.* **50** 1949–52
De Crescenzi M and Chiarello G 1985 *J. Phys. C: Solid State Phys.* **18** 3595–614
De Crescenzi M, Chiarello G, Colavita E and Memeo R 1984 *Phys. Rev.* B **29** 3730–2
De Crescenzi M, Chiarello G, Colavita E and Rosei R 1982 *Solid State Commun.* **44** 845–7
De Crescenzi M, Diociaiuti M, Lozzi L, Picozzi P and Santucci S 1987 *Phys. Rev.* B **35** 5997–6003
De Crescenzi M, Lozzi L, Picozzi P, Santucci S, Benfatto M and Natoli C R 1989 *Surf. Sci.* **211–212** 534–43
De Crescenzi M, Papagno L, Chiarello G, Scarmozzino R, Colavita E, Rosei R and Mobilio S 1981 *Solid State Commun.* **40** 613–7
Derrien J, Chainet E, De Crescenzi M and Noguera C 1987 *Surf. Sci.* **189–190** 590–604
Ekardt W E and Tran Thoai D B 1983 *Solid State Commun.* **45** 1083–4
Hitchcock A P and Teng C H 1985 *Surf. Sci.* **149** 558–76
Idzerda Y U, Williams E D, Einstein T L and Park R L 1985 *Surf. Sci.* **160** 75–86
—— 1987a *J. Vac. Sci. Technol.* A **5** 847–51
—— 1987b *Phys. Rev.* B **36** 5941–8
Lee P A and Beni G 1977 *Phys. Rev.* B **15** 2862–83
Mila F and Noguera C 1986 *J. Physique Coll.* **47** C8 339–542
—— 1987 *J. Phys. C: Solid State Phys.* **20** 3863–73
Natarajan C, Abel P B and Hoffman R W 1985 *J. Vac. Sci. Technol.* A **3** 1309–11
Papagno L and Caputi L S 1984 *Phys. Rev.* B **29** 1483–6
Papagno L, Caputi L S, Chiarello G and Delogu P 1986 *Surf. Sci.* **175** L767–72
Papagno L, De Crescenzi M, Chiarello G, Colavita E, Scarmozzino R, Caputi L S and Rosei R 1982 *Surf. Sci.* **117** 525–532
Polizzi S, Antonangeli F, Chiarello G and De Crescenzi M 1984 *Surf. Sci.* **136** 555–70
Rosei R, De Crescenzi M, Sette F, Quaresima C, Savoia A and Perfetti P 1983 *Phys. Rev.* B **28** 1161–4
Sayers D E, Stern E A and Lytle F W 1971 *Phys. Rev. Lett.* **27** 1204–7
Stern E A 1986 *J. Physique Coll.* **47** C8 3–10
Teng C H and Hitchcock A P 1983 *J. Vac. Sci. Technol.* A **1** 1209–10
Teo B K and Lee P A 1979 *J. Am. Chem. Soc.* **101** 2815–32
Teo B K, Lee P A, Simons A L, Einsenberg P and Kincaid B K 1977 *J. Am. Chem. Soc.* **99** 3854–6
Tyliszczak T and Hitchcock A P 1986 *J. Vac. Sci. Technol.* A **4** 1372–5